LIMNOLOGY and OCEANOGRAPHY

ASLO

Limnol. Oceanogr. 9999, 2023, 1–12

doi: 10.1002/lno.12301

Mechanistic understanding of diazotroph aggregation and sinking: "A rolling tank approach"

Fatima-Ezzahra Ababou,[1*] **Frédéric A. C. Le Moigne**,[1,2] **Olivier Grosso**,[1] **Catherine Guigue**,[1] **Sandra Nunige**,[1] **Mercedes Camps**,[1] **Sophie Bonnet**[1*]

[1]Aix Marseille Univ, Université de Toulon, CNRS, IRD, M.I.O UM 110, Marseille, France
[2]LEMAR, Laboratoire des Sciences de l'Environnement Marin, UMR6539, CNRS, UBO, IFREMER, IRD, Plouzané, Technopôle Brest-Iroise, France

Abstract

Diazotrophs are ubiquitous in the surface (sub)tropical ocean, where they sustain most new primary production. Several recent studies also report the presence of diverse cyanobacterial diazotrophs in the mesopelagic and bathypelagic ocean, suggesting that they gravitationally sink, potentially supporting organic matter export and the biological carbon pump. Yet, the mechanisms leading to their export are not elucidated. Here, we simulated the sinking of diazotrophs in the water column by using rolling tanks, and measured the aggregation capacity and sinking velocities of four globally distributed strains having different sizes, shapes, and abilities to produce transparent exopolymer particles (TEP): two filamentous diazotrophs (*Trichodesmium erythraeum*, *Calothrix* sp.) and two unicellular cyanobacterial diazotrophs (UCYN-B, *Crocosphaera watsonii*) and (UCYN-C, *Cyanothece* sp.). All diazotrophs tested, regardless their size and shape, were capable of forming aggregates and sunk, albeit at different velocities depending on the aggregation capacity. Overall, UCYN formed aggregates as large as those formed by the filamentous diazotrophs (7000–32,014 μm ESD, equivalent spherical diameter), and sunk at 100–400 m d^{-1}, i.e., at the same velocity as filamentous diazotrophs (92–400 m d^{-1}). Although TEP are generally considered as enhancers of aggregation, TEP did not clearly influence aggregation rates nor sinking velocities during our study. We conclude that diazotrophs may be important contributors to carbon export in the ocean and need to be considered in future studies to improve the accuracy of current regional and global estimates of export.

Primary productivity is limited by nitrogen (N) availability in the vast (sub)tropical ocean (Moore et al. 2013). In these N-depleted regions, dinitrogen (N_2) fixation performed by diazotrophs accounts for the major external source of new N (Gruber and Galloway 2008). This diazotroph-derived N is transferred to non-diazotrophic phyto, zooplankton, and bacteria (Berthelot et al. 2016; Bonnet et al. 2016; Caffin et al. 2018), which are then exported to the deep ocean, a process commonly called N_2-primed prokaryotic carbon pump (Karl et al. 2003). N_2 fixation may also influence the export of organic carbon directly through the gravitational settling of diazotrophs themselves, although few studies have focused on this pathway (Karl et al. 2012; Farnelid et al. 2019; Bonnet et al. 2022). Considering both direct and indirect export pathways, geochemical $\partial^{15}N$ budgets report that N_2 fixation accounts for ~25–50% of export production in the subtropical North Pacific (Station ALOHA, Hawaii) (Karl et al. 1998; Böttjer et al. 2017), ~10% in the subtropical North Atlantic (BATS) (Knapp et al. 2005), and 50–80% in the subtropical South Pacific (Knapp et al. 2018). However, the mechanisms leading to the export of diazotroph-derived biomass are not yet elucidated; in particular, our knowledge on direct export pathways remains obscure.

Diazotrophs exhibit a wide range of sizes, morphologies, and lifestyles. They can either be (i) small sized (2–8 μm in diameter) spherical/ovoid unicellular cyanobacteria (UCYN) either living freely (Groups B and C) (Zehr et al. 2001), or in

*Correspondence: fatima.ababou@mio.osupytheas.fr, sophie.bonnet@mio.osupytheas.fr

Additional Supporting Information may be found in the online version of this article.

Author Contribution Statement: F.E.A., S.B., and F.A.C.L.M. designed and performed the experiments with the help of M.C. F.E.A., O.G., C.G., and S.N. analyzed the samples. F.E.A., S.B., and F.A.C.L.M. analyzed the data and F.E.A prepared the manuscript with contributions of all co-authors.

symbiosis with coccolithophorids (UCYN-A, ~1 μm), (ii) large filamentous non-heterocystous cyanobacteria (>100–1000 μm) such as *Trichodesmium* sp. (Capone et al. 1997) with an elongated shape, or (iii) filamentous heterocystous diazotrophs (*Richelia* sp., *Calothrix* sp., ~10 μm) either living freely but often associated with ballasted diatoms (i.e., equipped with heavily silicified cell walls) and forming diatom–diazotroph associations (Villareal 1991). Finally, diazotrophs can also be non-cyanobacterial, including bacteria (Moisander et al. 2014; Bombar et al. 2016) and archaea (Loescher et al. 2014). These contrasted characteristics in terms of size, morphology, association, or not with ballasting minerals may influence the fate of diazotrophs in the ocean (Jackson 1990; Le Moigne et al. 2013; Iversen and Robert 2015). However, the potential for diazotrophs to directly sink to the deep ocean has rarely been studied.

Most of our knowledge is based on diatom–diazotroph associations, which play an important role in organic carbon export (Subramaniam et al. 2008; Karl et al. 2012; White et al. 2013) and generate summer export pulses down to 4000 m at Station ALOHA near Hawaii (Karl et al. 2012). Despite its large size, *Trichodesmium* sp. has long been considered to be poorly exported and preferentially remineralized in surface waters (Walsby 1978; Mulholland 2007). This is due to its buoyancy provided by gas vesicles (Walsby 1978) and to the minimized production of ballast associated with glycogen utilized as an energy store for nitrogenase (Held et al. 2022). Intact *Trichodesmium* sp. colonies have however been detected in the mesopelagic (200–1000 m) (Bonnet et al. 2022; Benavides et al. 2022), and bathypelagic ocean (>1000 m depth) in the subtropical North Atlantic, Pacific, and Indian oceans (Agusti et al. 2015; Pabortsava et al. 2017; Poff et al. 2021). Fewer data are available on the export of UCYN despite their high abundances and significant role in N dynamics in the global ocean (Zehr et al. 2001; Luo et al. 2012). UCYN are deemed to contribute little to direct carbon export because of their small size (~4–8 μm) and thus assumed slow sinking velocity (Bach et al. 2012), likely leading to rapid remineralization. Recent studies, however, report the presence of UCYN-B and UCYN-C in mesopelagic waters of the subtropical North and South Pacific (Caffin et al. 2018; Farnelid et al. 2019; Bonnet et al. 2022). UCYN from Groups A, B, and C seem to be exported more efficiently than *Trichodesmium* sp. in the subtropical South Pacific ocean (Bonnet et al. 2022). UCYN were indeed found embedded in large (50–2000 μm) aggregates linked by Extracellular Polymeric Substances (EPS). In fact, *Crocosphaera watsonii* (UCYN-B) produces twice as much EPS as diatoms and coccolithophores (Sohm et al. 2011), and *Trichodesmium* sp. synthetizes large quantities of a sub-category of EPS, i.e., a sticky and carbon-rich particles termed transparent exopolymer particles (TEP) (Passow 2000; Berman-Frank et al. 2007). TEP are recognized as a major element of carbon cycling and export in marine environments (Passow and Alldredge 1995; Mari and Burd 1998; Passow 2002) as they promote particle aggregation (Engel 2004; Mari et al. 2017). However, whether TEP produced by diazotrophs support their aggregation and sinking or cause them to float is still unclear (Mari et al. 2017). As the density of TEP is lower than that of seawater (700–840 kg m^{-3} vs. 1020–1030 kg m^{-3}), this may lead to an ascending rather than descending flow of diazotroph aggregates if they are not ballasted (Azetsu-Scott and Passow 2004).

Collectively, these results indicate that diazotrophs of different sizes, morphologies and lifestyles have the potential to directly sink below the photic layer. However, export mechanisms remain understudied. In particular, the aggregation rate and sinking velocities of diazotrophs having different sizes, shapes, and abilities to produce TEP need to be investigated. Here we used rolling tanks to physically simulate the sinking of diazotrophs in the water column. We measured the aggregation rate and sinking velocities of aggregates formed by four contrasted diazotrophs grown in culture, to explore their potential to export organic matter.

Materials and methods

Diazotroph cultures

Four subtropical cyanobacterial diazotrophs were selected (Table S1): (i) the filamentous non-heterocystous strain *Trichodesmium erythraeum* IMS101 (hereafter *Trichodesmium*), (ii) the filamentous heterocystous strain *Calothrix* sp. (hereafter *Calothrix*), (iii) the UCYN from Group B, *C. watsonii* WH0003 (hereafter UCYN-B), and (iv) a UCYN from Group C, *Cyanothece* sp. (hereafter UCYN-C). Both UCYN strains produce approximatively twice as much TEP per unit of C than filamentous strains (Table S1).

Cultures were grown in a thermostat-controlled room at 27°C in a 12 : 12-h light–dark cycle under a 120 μmol photons m^{-2} s^{-1} irradiance. Strains were grown in sterile 10 L autoclaved glass bottles; 14 L of each strain were necessary for each experiment. The culture medium was composed of 0.2 μm-filtered natural seawater characterized by low nitrate concentrations (<0.1 μM), autoclaved, and amended with nutrients in the same proportion as for the YBCII medium (Chen et al. 1996) (*see* SI for the YBCII recipe).

Experimental setup

At the end of the exponential growth phase, cultures were transferred to custom-made 3.45 L rolling tanks. Because rolling tanks were filled to the top avoiding air-bubbles that induce strong shear, solid body rotation was established, thus maintaining particles in suspension and simulating their sinking in the water column (Ploug et al. 2010). Each strain was studied in duplicate rolling tanks and in two different conditions (4 tanks per strain): for each tank, two thirds were filled with the diazotroph culture, and one third with natural seawater collected at an oligotrophic station (Mediterranean Sea,

43°14′30″ N; 5°17′30″ E), which was either (i) 0.2 μm-filtered (hereafter filtered seawater) to remove phytoplankton, microzooplankton, and bacteria, or (ii) unfiltered (hereafter natural seawater). These two treatments were performed to test whether the presence of living plankton in the natural seawater conditions enhance or not aggregation. We paid attention to introduce approximatively the same number of cells (10^5 cells L^{-1} for UCYN) or biomass in the tanks at the beginning of the experiment to be able to compare the strains between them. Unlike UCYN and *Trichodesmium*, *Calothrix* cannot be easily counted, so we weighed dry matter and introduced 2×10^4 μg L^{-1} of biomass for *Calothrix* and thus did the same for *Trichodesmium*.

Rolling tanks were maintained in darkness at 20°C (average temperature of the subtropical ocean where these diazotrophs thrive—at the base of the photic layer) at 3 rotations per minute for 4 d. At Days 2, 3, and 4, each tank was carefully removed from the table, placed on its base and photographed (*see* below) before being replaced on the roller table taking care not to break the aggregates. Sampling inside the tanks was performed at Day 0 (before sealing and installing the tanks in the roller table) and at Day 4 (at the end of the experiment). All samples were systematically collected in three technical replicates from each duplicate tank and from two fractions: aggregates and water (containing non-aggregated cells). For this purpose, the tanks were placed under a laminar flow hood for 10 min, allowing aggregates to settle. We first collected water for the following parameters: dissolved and particulate organic carbon (DOC and POC), particulate organic nitrogen (PON), nitrate + nitrite (NO_x) and phosphate (PO_4^{3-}) concentrations and TEP content. Some aggregates were sampled for sinking velocity measurements and the rest was gently collected with a syringe attached to a pipette and pooled in a single cleaned Schott flask before subsampling for the same parameters as above except DOC.

Analyses

Aggregates abundance, size, and morphology

Changes in abundance, size, and morphological properties of aggregates were assessed by imaging the particles formed in the tanks. Tanks were gently removed from the roller table and placed on a plexiglass cold light illuminated plate for 5 min to improve the image quality and to allow aggregates to sink to the bottom of the tanks. Pictures (Pentax K20 camera) were analyzed using FIJI (Image J) (Schindelin et al. 2015). With the threshold function, pictures were converted into binary images (black and white) to measure the shape descriptors (area, angle, circularity, perimeter, fit ellipse, and aspect ratio) of particles. Particle size spectra were obtained from the equivalent spherical diameter (ESD) of particles binned into 15 logarithmically spaced size classes (Table S2) (Laurenceau-Cornec et al. 2019) covering the whole size range (176–32,014 μm ESD). Bins containing few particles were not excluded from the analysis due to the formation of a large and single (or few) aggregates in some of the tanks (Fig. 1). Aggregates of a circularity of 1 positioned at specific angles (0°, 45°, 90°, 135°, and 180°) were considered as spurious aggregates and were therefore excluded from the dataset. This cut-off removed a minor number of aggregates.

Dissolved and particulate organic carbon and nitrogen

Samples for POC and PON concentrations were collected in three technical replicates from each duplicate tank. They were filtered onto pre-combusted (450°C, 6 h) GFF filters and dried at 55°C before analysis using an elemental analyzer coupled to an isotope ratio-mass spectrometer (EA-IRMS, Integra 2) (Bonnet et al. 2018). POC data were used to estimate the aggregation capacity (percentage of aggregation) of diazotrophs, i.e., the fraction of POC transferred from the water to the aggregates fraction during the 4 d of the experiment. DOC samples were collected in three technical replicates, filtered under a laminar flow hood through a 0.2 μm Sartobran (Sartorius) cartridge connected to a peristaltic pump, transferred into a pre-combusted (450°C, 6 h) 10 mL glass vials, and fixed with 20 μL of HCl (37%). Samples were stored at 4°C in the dark until analyses using a Shimadzu TOC–V analyzer (Guigue et al. 2017).

Sinking velocity measurements

Aggregate sinking velocities were measured by following their trajectory while sinking through a 6 L transparent Plexiglas cylinder of 15 cm diameter and 46 cm height as described in Riley et al. (2012). The cylinder was filled using medium with the same water properties and temperature as used in the rolling tanks. Multiple aggregates from each tank (12 of *Trichodesmium*, 5 of *Calothrix*, 4 of UCYN-B, and 12 of UCYN-C) were gently collected into a dedicated 50 mL pipette whose tip had been cut off and released by gravity below the water surface in the sinking cylinder. The sinking time was measured once the aggregate speed was stabilized in the column and was measured only once due to the extreme fragility of the aggregates. Sinking time was then converted to sinking velocities in meters per day (Riley et al. 2012).

Microscopic determination of TEP content

TEP were stained as described in Passow and Alldredge (1995). Briefly, duplicate 3 mL of tank water or aggregates were filtered onto 0.4 μm pore size 25 mm diameter polycarbonate filters (Nuclepore, Poretics) at a constant and low vacuum pressure (<150 mmHg) to not damage TEP. Damp filters were then stained for 5 s with 1 mL of pre-filtered 0.2 μm Alcian Blue solution (0.02% aqueous solution, 0.06% acetic acid, pH 2.5) and rinsed with 5 mL of MilliQ water to remove excess dye. The dry stained filters were soaked in immersion oil (Cargille Laboratories, 1460–1640 ± 0.002, ND = 1.584) (Freibott et al. 2014), placed onto transparent slides and stored at −20°C until analysis. 8 blank filters were also stained with Alcian Blue and rinsed with MilliQ water.

Filters were thawed at room temperature and photographed at a 100× magnification using an epifluorescence microscope

(Zeiss Axioplan, white light) equipped with a camera, following a vertical and a horizontal transect across the whole filter (Engel 2009). After analyzing all images in FIJI (script in the SI), the original and binary images were visually compared to ensure that the threshold included only the stained TEP. The TEP content expressed in mm^2 μmol C^{-1} of POC was obtained by calculating TEP area per volume of sample (mm^2 L^{-1}) normalized by the corresponding POC concentrations (μmol C L^{-1}).

Results

Diazotroph aggregates

Direct observation of the tanks provides a preliminary indication of the aggregation dynamics of diazotrophs during the experiment (Fig. 1). Aggregates of sizes ranging from 176 to 32,014 μm ESD were formed similarly in both natural and filtered seawater conditions within hours from the start of the rotation. One aggregate of *Calothrix* and one of UCYN-C were larger than this size range (24,520 and 172,000 μm ESD, respectively) and are not presented in the data.

Between Day 1 (24 h) and Day 4 (96 h), *Trichodesmium* increasingly formed visible aggregates of different sizes. Surprisingly, *Calothrix* aggregated within an hour and formed a single, large and compact aggregate. UCYN-B formed compact aggregates alike to long entangled filaments, whereas UCYN-C formed at Day 1 relatively few medium-sized aggregates that aggregated further at Day 4 to form larger aggregates (Fig. 1).

At Day 2, small aggregates (176–732 μm ESD) were more abundant in the tanks containing *Trichodesmium* and UCYN-B, compared to the tanks containing *Calothrix* and UCYN-C (Fig. 2). At Day 3, the abundance of small aggregates decreased by 6-, 3-, and 2-fold in the tanks containing *Trichodesmium*, *Calothrix* and UCYN-B, respectively, but increased by 6-fold in the tanks containing UCYN-C compared to Day 1. At Day 4, they decreased (by 2- and 3-fold, respectively) in the *Calothrix* and UCYN-C tanks, while very small aggregates (size range 176–359 μm ESD) appeared in the *Trichodesmium* and UCYN-B tanks, likely due to disaggregation. Conversely, the abundance of large (7000–32,014 μm ESD) aggregates increased by 2.5-fold in the *Trichodesmium* tanks between Day 2 and Day 4, whereas no change was observed for *Calothrix* single aggregate. For UCYN, the abundance of this size range of aggregates did not change between Day 2 and 4 for UCYN-C and increased by 3.5-fold for UCYN-B.

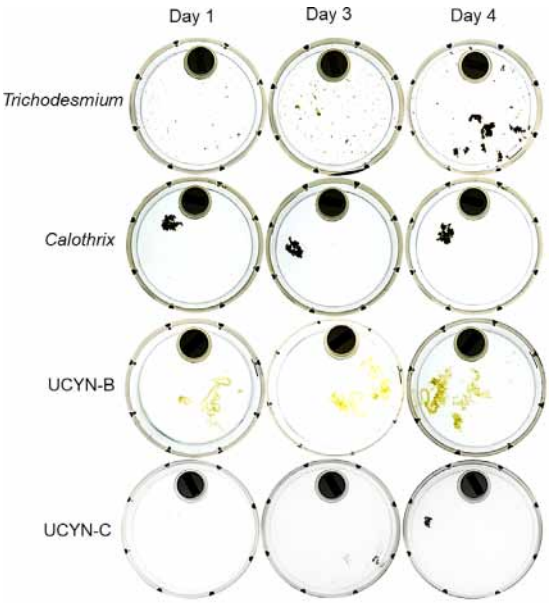

Fig. 1. Photographs of aggregates formed in the rolling tanks (natural seawater condition) for each diazotroph tested after 24 h (Day 1), 72 h (Day 3) and 96 h (Day 4) of rotation on the roller table.

Overall, all diazotrophs tested formed large aggregates (12,761–32,014 μm ESD) in both conditions. Small aggregates (176–359 μm ESD) were 20, 12, and 9 times more numerous in natural compared to filtered seawater conditions for *Trichodesmium*, UCYN-C, and UCYN-B, whereas they were twice less numerous for *Calothrix* (Fig. 2).

Aggregation capacity, carbon budget, and sinking velocities

Two distinct fractions formed during the simulated sinking: the aggregate fraction, and the water fraction (containing non-aggregated cells). POC concentrations in the water fraction (average natural and filtered seawater conditions) decreased by $86 \pm 4\%$ for *Calothrix*, $70 \pm 2\%$ for UCYN-B, $68 \pm 4\%$ for *Trichodesmium* and $48 \pm 1\%$ for UCYN-C between Day 0 and Day 4 (Fig. 3), while POC was transferred to the aggregate fraction. The aggregation capacity (the fraction of POC transferred from the water to the aggregates during the 4 d of the experiment) significantly differed among the strains tested (Kruskal–Wallis test, $p = 0.0001$), with $62 \pm 13\%$ for *Calothrix*, $43 \pm 1.2\%$ for UCYN-B, $31 \pm 0.6\%$ for UCYN-C, and $18 \pm 6.2\%$ for *Trichodesmium* (Fig. 4) (average natural and filtered seawater conditions). *Trichodesmium* and *Calothrix* aggregated more efficiently in the filtered ($23 \pm 2\%$ and $74 \pm 21\%$, respectively) than in the natural seawater conditions ($14 \pm 2\%$ and $54 \pm 11\%$) (Mann–Whitney test, $p = 0.002$), whereas it was not the case for both UCYN strains tested (Mann–Whitney test, $p = 0.486$) (average seawater conditions: $43 \pm 1\%$ for UCYN-B and $31 \pm 0.6\%$ for UCYN-C).

PON concentrations in the water fraction (average natural and filtered seawater conditions) decreased by $72 \pm 7\%$ for *Calothrix* between Day 0 and Day 4, $62 \pm 4\%$ for UCYN-B, $46 \pm 7\%$ for *Trichodesmium* and $41 \pm 0.3\%$ for UCYN-C, while PON was transferred to the aggregate fraction. The resulting C : N ratios at Day 0 (averages of the two seawater conditions) were 6.1 ± 0.1 mol mol^{-1} for *Trichodesmium*, 9.1 ± 0.4 mol mol^{-1} for *Calothrix*, 12.8 ± 0.1 mol mol^{-1} for UCYN-B and 12.4 ± 0.1 mol mol^{-1} for UCYN-C (Fig. 5). In

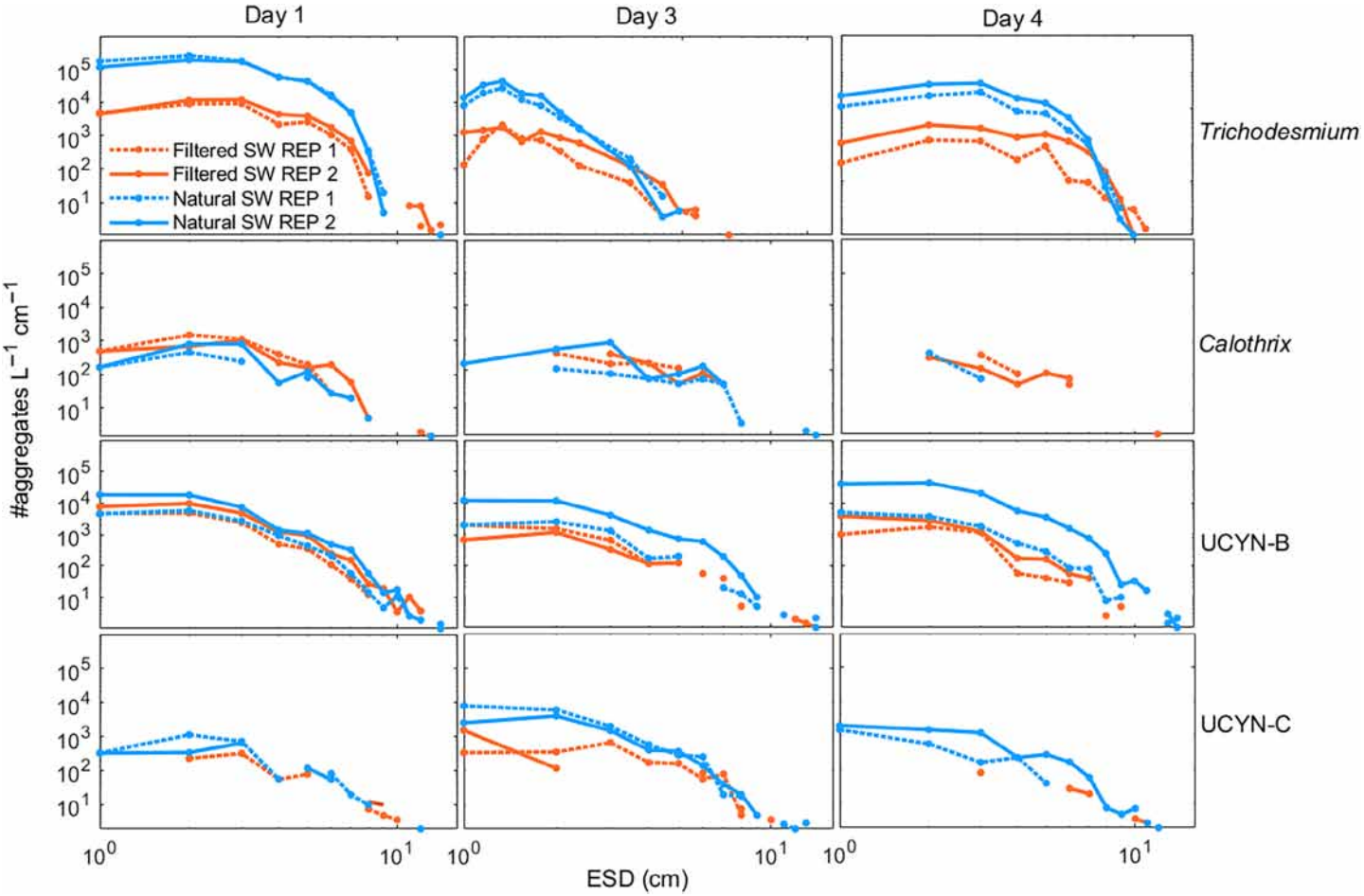

Fig. 2. Size spectra of diazotroph aggregates formed in the duplicate tanks at Day 1, Day 3 and Day 4, binned into 15 size classes (replicate 1: dashed lines and replicate 2: solid lines) in natural seawater (blue) and filtered seawater (orange).

the aggregate fraction, the C : N ratios at Day 4 decreased significantly (Mann–Whitney test, $p = 0.02$), by $17 \pm 2.5\%$ for *Trichodesmium*, $22 \pm 1\%$ for UCYN-B and $8 \pm 3.2\%$ for UCYN-C, and remained constant for *Calothrix* (average C : N ratio of 9.2 ± 0.1 mol mol^{-1} between Day 0 and Day 4). In the water fraction, the changes in the C : N ratios at Day 4 followed the same trend as those of the aggregates with a decrease of $22 \pm 3\%$ for *Trichodesmium*, $41 \pm 1\%$ for *Calothrix*, $21 \pm 2\%$ for UCYN-B, and $13 \pm 1\%$ for UCYN-C.

DOC concentrations did not vary significantly (Mann–Whitney test, $p = 0.19$) between Day 0 and 4 for all strains and conditions tested. We thus found a "loss" of organic carbon (OC) in all the tanks between initial and final POC and DOC stocks that we considered as a "remineralized" fraction due to the presence of bacteria (Fig. 3). This loss (average of the two seawater conditions) was of $36 \pm 5\%$, $21 \pm 4\%$, $17 \pm 14\%$, and $9 \pm 1\%$ in the *Trichodesmium*, UCYN-B, *Calothrix* and UCYN-C tanks, respectively. It was not significantly different between the two conditions for all strains tested (Mann–Whitney test, $p = 0.13$) (Fig. 3).

Calothrix aggregates exhibited the highest sinking velocities (433 ± 157 m d^{-1}) followed by UCYN-B (408 ± 172 m d^{-1}), UCYN-C (102 ± 54 m d^{-1}), and *Trichodesmium* aggregates (92 ± 37 m d^{-1}) (Fig. 6). It has to be noted that some of the *Trichodesmium* aggregates tested had a positive buoyancy and did not sink. Sinking velocities of diazotrophs were positively correlated with their aggregation capacity (Fig. S1a, $R^2 = 0.8$), suggesting that the more diazotrophs aggregated the faster they sunk.

TEP content

The initial TEP content (average natural and filtered seawater conditions) was 7.6 ± 1, 4.7 ± 1, 3.4 ± 0.1, and 2.7 ± 0.5 mm^2 μmol C^{-1} in the tanks containing UCYN-B, UCYN-C, *Calothrix*, and *Trichodesmium*, respectively (Fig. 7), with no significant difference between the two conditions (Mann–Whitney test, $p = 0.052$). The final TEP content in the aggregate fractions (average natural and filtered seawater conditions) increased by 5 ± 4.6, 2 ± 0.3, 2 ± 0.4, and 1.3 ± 0.6 fold for *Trichodesmium*, UCYN-C, *Calothrix*, and UCYN-B,

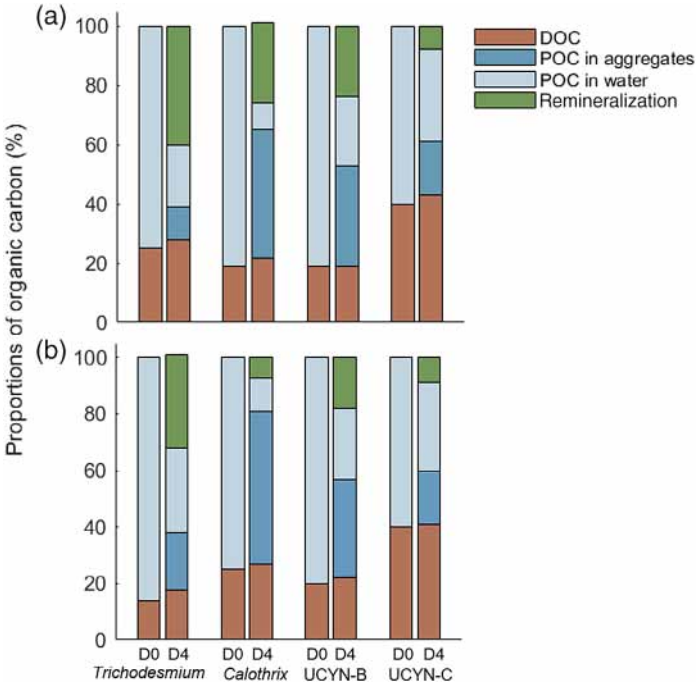

Fig. 3. Proportions of DOC (brown), POC in aggregates (blue), POC in water (light blue) and carbon loss (estimation of remineralization) (green) in (**a**) natural and (**b**) filtered seawater conditions. Proportions of each fraction are calculated at Day 0 (D0) and Day 4 (D4) as follows: Concentration of the fraction considered (μmol)/TOC × 100. Standard deviations are < 2% and are given in Table S3.

respectively (Fig. 7). It was 5, 2 and 1.4-fold higher in the natural than in the filtered seawater conditions for *Trichodesmium*, UCYN-B and *Calothrix*, whereas they were 1.3-fold higher for UCYN-C in filtered seawater conditions.

The final TEP content released in the water fraction (average natural and filtered seawater conditions) was 12 ± 3, 11 ± 8, 10 ± 2, and 4 ± 2 mm^2 μmol C^{-1} POC for UCYN-C, *Trichodesmium*, UCYN-B, and *Calothrix*, respectively. It was higher in the natural seawater conditions for *Trichodesmium* due to the burst of some of the trichomes (Figs. 7, 8).

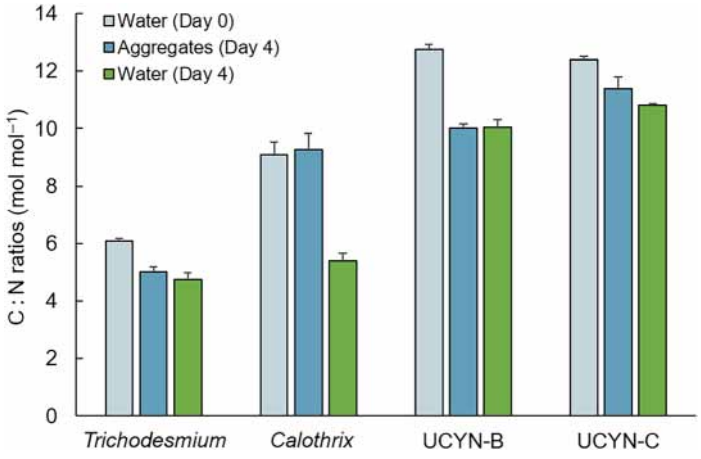

Fig. 5. Particulate C : N ratio (POC : PON, mol mol^{-1}) in average natural and filtered seawater conditions in the water fraction at Day 0 (light blue) and at Day 4 (green), and in the aggregates fraction (blue).

Discussion

Aggregation dynamics and sinking

Here we show that all diazotrophs tested, regardless their size and shape (e.g., UCYN or filamentous) are capable of forming aggregates and sinking (Figs. 1, 6), albeit at different velocities depending on their aggregation capacity. Overall, UCYN formed aggregates as large as those formed by filamentous diazotrophs (Fig. 2), and sunk at 100–400 m d^{-1}, i.e., at the same velocity as filamentous diazotrophs (92–400 m d^{-1}). This shows that, although UCYN are smaller than filamentous, once aggregated, they both form aggregates of similar size (Fig. 2) and sink at similar velocities, or even faster than *Trichodesmium* (Fig. 6). This result is consistent with a recent in situ study revealing that both *Trichodesmium* and UCYN groups sink to the deep ocean (1000 m) throughout the subtropical ocean (Bonnet et al. 2022). They also found that UCYN sink more efficiently than *Trichodesmium* (the export turnover rates of UCYN were approximately four times higher than those of *Trichodesmium*) due to aggregation of small UCYN in large and dense aggregates.

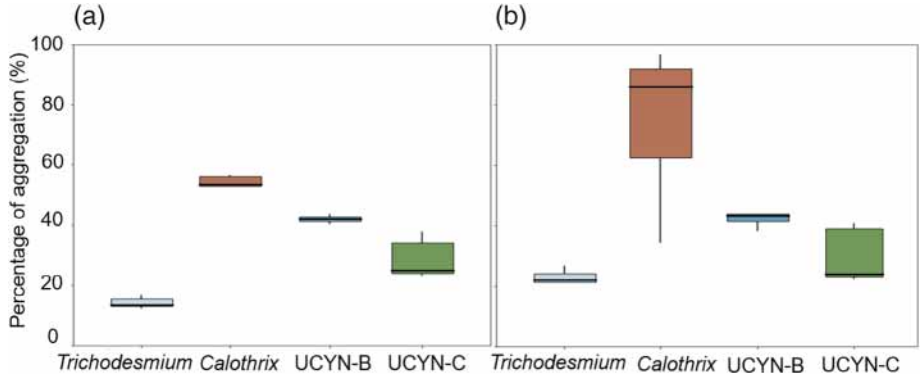

Fig. 4. Percentage of aggregation of diazotrophs in (**a**) natural and (**b**) filtered seawater calculated as the ratio of POC in aggregates at Day 4 over total POC at Day 0 (% aggregation = [POC in aggregates at Day 4 × 100]/POC at Day 0).

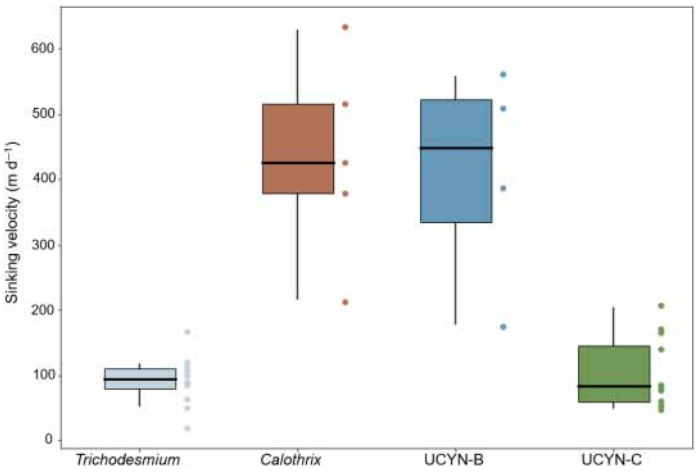

Fig. 6. Average sinking velocity of diazotroph aggregates in meters per day for *Trichodesmium* ($n = 12$ aggregates), *Calothrix* ($n = 5$ aggregates), UCYN-B ($n = 4$ aggregates) and UCYN-C ($n = 12$ aggregates) collected from both natural and filtered seawater conditions.

For all diazotrophs tested, the POC was transferred from the water to the aggregate fraction within hours to days, suggesting that part of the diazotrophs suspended in seawater have aggregated, by 18 ± 6 to 62 ± 13%, depending on diazotroph species (Fig. 4). One potential explanation for the *Calothrix* exceptional aggregation (62 ± 13%) is its ability to form visible small aggregates even in culture. Its entangled filaments likely facilitated its aggregation (Table S1). One must note that among all the marine diazotrophs tested, *Calothrix* originates from a coastal region (coral lagoon ecosystem), whereas others were isolated from the open ocean. When considering only oceanic strains, we find that UCYN have a higher aggregation capacity (43 ± 1% for UCYN-B and 31 ± 1% for UCYN-C) than *Trichodesmium* (18 ± 6%) (Fig. 4).

All diazotrophs tested here in vitro sunk at velocities ranging from 92 to 433 m d^{-1} (Fig. 6), and one can wonder if such values reflect actual in situ sinking velocities. Laurenceau-Cornec et al. (2015) compared natural aggregates collected in gel traps with artificially-produced aggregates from natural seawater coming from the same site (Kerguelen Plateau) in rolling tanks. The structure and fractal size of both natural and artificial aggregates were similar. As these two parameters influence the sinking of particles (Johnson et al. 1996), we are confident that sinking velocities reported here are likely to reflect in situ velocities.

As stated above, the large size, and the seemingly high compactness/density of *Calothrix* aggregates may explain their high sinking velocity (433 ± 157 m d^{-1}). Both UCYN-B and UCYN-C sunk faster (408 ± 172 and 102 ± 54 m d^{-1}, respectively) than *Trichodesmium* (92 ± 37 m d^{-1}) (Fig. 6). This is likely due to the formation of UCYN aggregates, which are larger, and look less fragile and denser than those of *Trichodesmium* (Fig. 1), probably because UCYN-B produce high quantities of glycogen acting as a ballast (Held et al. 2022). Unlike UCYN-B fixing N_2 at night, *Trichodesmium* minimizes its glycogen production by fixing N_2 during daylight, directly providing energy to the nitrogenase, but reducing cell-specific mass density and thus likely decreasing its sinking velocity (Held et al. 2022). Further studies would be required to measure aggregates excess density and better elucidate the differences observed in sinking velocities among the diazotrophs tested. The relatively low sinking velocity of *Trichodesmium* (Fig. 6) is also likely due to its low aggregation capacity and to its natural buoyancy due to gas vesicles. The vast majority (up to 100%) of gas vesicles generally collapse between 105 and 120 m (Walsby 1978). In our study, we simulated a descent down to ~ 400 m depth (by considering 92 m d^{-1}), but in the absence of hydrostatic pressure, it is likely that gas vesicles were still present, further decreasing the sinking velocity of the formed aggregates. Additionally, autocatalytic programmed cell death (PCD) processes may have been activated in the rolling tanks due to the aging of trichomes (Berman-Frank et al. 2007; Bar-Zeev et al. 2013), likely

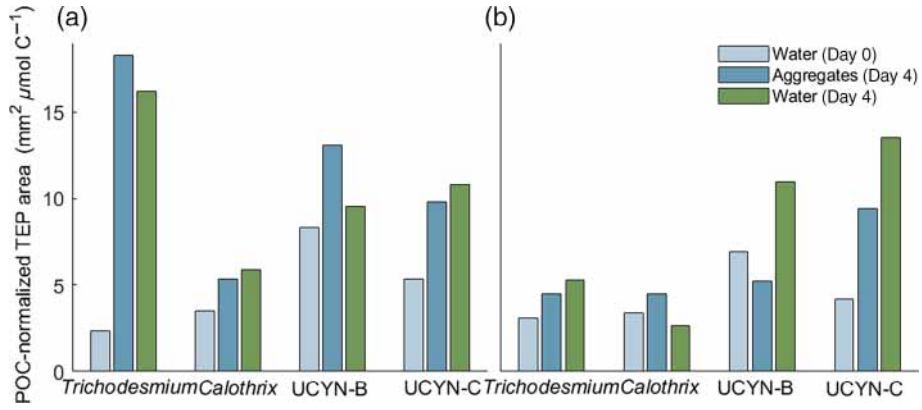

Fig. 7. TEP content expressed in POC-normalized TEP area (mm² µmol C^{-1} POC) in (**a**) natural and (**b**) filtered seawater conditions, in the water fraction at Day 0 (light blue) and Day 4 (green), and in the aggregates at Day 4 (blue).

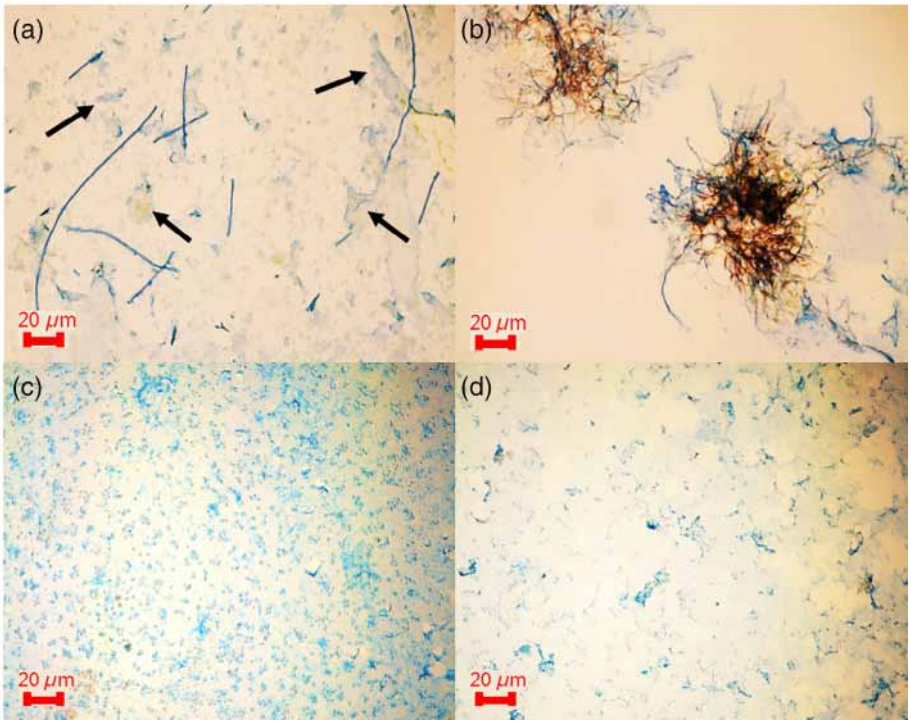

Fig. 8. Microscopic observations of TEP in the different diazotroph aggregates formed in natural seawater conditions. The blue color corresponds to TEP stained by Alcian Blue. (**a**) *Trichodesmium* filaments with some bursted trichomes pointed by black arrows (**b**) *Calothrix* with TEP mostly located at the outer edge of the aggregates (**c**) UCYN-B and (**d**) UCYN-C with TEP both attached to the cells and released in the seawater.

resulting in our observations: large sinking aggregates of *Trichodesmium* (the ones that lost gas vesicles) and small non-sinking aggregates. PCD likely triggered the production of TEP (Berman-Frank et al. 2007), reducing the aggregate density (Mari et al. 2017) and in turn, the sinking velocity. This hypothesis is the most plausible as the highest TEP production was observed for *Trichodesmium* in natural seawater conditions where trichomes burst and released their material and TEP concentrations increased 5-fold between Day 0 and Day 4 (Figs. 7, 8).

Role of TEP in diazotroph aggregation and sinking

TEP are considered as one of the major factors influencing aggregation (Engel 2000; Passow 2002). However, they can also potentially reduce aggregate sinking velocities due to their low density (Kiørboe et al. 1998; Mari et al. 2017). In our study, we found either (i) no correlation between TEP content and diazotroph aggregation, or (ii) negative correlations for *Trichodesmium* and *Calothrix* (Fig. S1c,d), i.e., they aggregated the most when the lowest TEP concentrations were measured. This shows that TEP did not systematically increase the aggregation of the diazotrophs tested. However, microscopic observations of TEP were carried out at a single magnification (100×), which may not cover all their size range. In future studies, capturing TEP at increasing magnifications (100×, 200× then 400×), including small TEP particles, would provide additional information about their role in diazotroph aggregation dynamics (Mari et al. 2005).

TEP promote aggregation when they are dense and highly sticky (Mari et al. 2017). However, TEP stickiness depends on several factors such as the source, the age of TEP, the bacterial activity, the temperature and pH of seawater (Mari et al. 2017). Likewise, light is known to decrease the TEP stickiness (Rochelle-Newall et al. 2010) (our tanks were incubated in the dark). Finally, the chemical composition of the TEP pool is complex as it depends on the organisms that produce them, meaning that TEP concentration may be similar but their chemical composition may differ substantially, which in turn may influence their stickiness.

C : N ratios of particulate organic matter

The averaged C : N ratios (mol mol^{-1}) at the start of the experiment ranged from 6.1 ± 0.1 for *Trichodesmium* to 12.8 ± 0.1 for UCYN-B (Fig. 5). Unlike *Trichodesmium*, that falls within the Redfield's stoichiometric observations, the C : N ratios of *Calothrix* (9.1 ± 0.4 mol mol^{-1}) and both UCYN (average 12.6 ± 0.2 mol mol^{-1}) were higher, but consistent with phytoplankton C : N ratios in oligotrophic regions (7.2–14.4 mol mol^{-1}) (Villareal and Carpenter 1994; Mari et al. 2017) and of diazotrophs (4.7–12 mol mol^{-1}) (Dekaezemacker and Bonnet 2011; Berthelot et al. 2015).

All C : N ratios in diazotroph aggregates decreased during the 4 d of simulated sinking, except for *Calothrix* (Fig. 5). The decrease in aggregate C : N ratios during sinking is reported here for the first time for tropical diazotrophs. We suggest four hypotheses to explain such a trend: (i) the particulate organic matter originated from diazotrophs may be composed of more proteins than carbohydrates; (ii) N_2 fixation of diazotrophs may have remained active during their simulated sinking (Bonnet et al. 2013; Benavides et al. 2022), leading to a potential increase of the N cell quota and a subsequent decrease of the C : N ratio; (iii) cultures were non axenic, which may have led to high abundance of bacteria having low C : N ratios (3.7–5.6 mol mol^{-1}) (Caron et al. 1995) within and around the diazotroph aggregates, further reducing the measured C : N ratios; and finally (iv) N became limiting in the tanks at the end of the experiment (Fig. S2), meaning that TEP formed in such conditions may have assimilated the dissolved nitrogenous compounds present in the medium, leading to a decrease of the C : N ratios of such TEP-rich aggregates (Mari 1999). These results therefore suggest that diazotrophs may export N deeper and more efficiently than C to the seafloor.

Considering our measured sinking velocities (92 and 400 m d^{-1}), diazotrophs would reach a depth of 1000 m in 2.5–11 d. This is sufficient to escape a complete remineralization and reach long-term C storage depth (sequestration depths, Baker et al. 2022). This estimate is consistent with in situ observations reporting the presence of intact *Trichodesmium* colonies and UCYN aggregates at 1000 m and below (Agusti et al. 2015; Pabortsava et al. 2017; Bonnet et al. 2022), sometimes alive at such depths (Benavides et al. 2022). Altogether, this suggests that diazotrophs, when sinking, sink fast enough to escape complete remineralization, and may contribute to C sequestration to the deep ocean.

Conclusion

It has long been assumed that the fate of diazotroph-derived biomass is mostly limited to surface waters. Our results challenge this assumption and show that the globally-distributed diazotrophs tested here sink and have the potential to export organic matter to the deep ocean, thus providing a step forward in defining the role of diazotrophs on the global carbon flux. All diazotrophs tested, regardless their size and shape are indeed capable of forming aggregates and sink at different velocities depending on the aggregation capacity. Small UCYN form aggregates as large as those formed by filamentous diazotrophs and sink at similar velocities. Although TEP are generally considered as enhancers of aggregation, TEP did not clearly influence aggregation rates nor sinking velocities during our study.

Some of the biogeochemical models predict an expansion of oligotrophic regions (where diazotrophs thrive) in future climate scenarios, due to enhanced seawater temperatures and stratification (Sarmiento et al. 2004; Hutchins and Fu 2017). In some scenarios (Bopp et al. 2022), N_2 fixation is likely to increase, further enhancing future new primary production. The data provided here will contribute to help our community to accurately parameterize, model and predict the role of diazotrophs on carbon sequestration in a warmer, more acidic, and more stratified future ocean.

Data Availability Statement

Not applicable.

References

Agusti, S., J. I. González-Gordillo, D. Vaqué, M. Estrada, M. I. Cerezo, G. Salazar, J. M. Gasol, and C. M. Duarte. 2015. Ubiquitous healthy diatoms in the deep sea confirm deep carbon injection by the biological pump. Nat. Commun. **6**: 1–8. doi:10.1038/ncomms8608

Azetsu-Scott, K., and U. Passow. 2004. Ascending marine particles: Significance of transparent exopolymer particles (TEP) in the upper ocean. Limnol. Oceanogr. **49**: 741–748. doi:10.4319/LO.2004.49.3.0741

Bach, L. T., U. Riebesell, S. Sett, S. Febiri, P. Rzepka, and K. G. Schulz. 2012. An approach for particle sinking velocity measurements in the 3–400 μm size range and considerations on the effect of temperature on sinking rates. Mar. Biol. **159**: 1853–1864. doi:10.1007/s00227-012-1945-2

Baker, C. A., A. P. Martin, A. Yool, and E. Popova. 2022. Biological carbon pump sequestration efficiency in the North Atlantic: A leaky or a Long-term sink? Global Biogeochem. Cycles. **36**: e2021GB007286. doi:10.1029/2021GB007286

Bar-Zeev, E., I. Avishay, K. D. Bidle, and I. Berman-Frank. 2013. Programmed cell death in the marine cyanobacterium Trichodesmium mediates carbon and nitrogen export. ISME J. **7**: 2340–2348. doi:10.1038/ismej.2013.121

Benavides, M., and others. 2022. Sinking Trichodesmium fixes nitrogen in the dark ocean. ISME J. **2022**: 1–8. doi:10.1038/s41396-022-01289-6

Berman-Frank, I., G. Rosenberg, O. Levitan, L. Haramaty, and X. Mari. 2007. Coupling between autocatalytic cell death and transparent exopolymeric particle production in the marine cyanobacterium *Trichodesmium*. Environ. Microbiol. **9**: 1415–1422. doi:10.1111/j.1462-2920.2007.01257.x

Berthelot, H., and others. 2015. Dinitrogen fixation and dissolved organic nitrogen fueled primary production and particulate export during the VAHINE mesocosm experiment (New Caledonia lagoon). Biogeosciences. **12**: 4099–4112. doi:10.5194/bg-12-4099-2015

Berthelot, H., S. Bonnet, O. Grosso, V. Cornet, and A. Barani. 2016. Transfer of diazotroph-derived nitrogen towards non-diazotrophic planktonic communities: A comparative study between *Trichodesmium erythraeum*, *Crocosphaera watsonii* and *Cyanothece* sp. Biogeosciences. **13**: 4005–4021. doi:10.5194/BG-13-4005-2016

Bombar, D., R. W. Paerl, and L. Riemann. 2016. Marine non-cyanobacterial diazotrophs: Moving beyond molecular detection. Trends Microbiol. **24**: 916–927. doi:10.1016/j.tim.2016.07.002

Bonnet, S., and others. 2016. Diazotroph derived nitrogen supports diatom growth in the South West Pacific: A quantitative study using nanoSIMS. Limnol. Oceanogr. **61**: 1549–1562. doi:10.1002/LNO.10300

Bonnet, S., and others. 2018. In-depth characterization of diazotroph activity across the western tropical South Pacific hotspot of N_2 fixation (OUTPACE cruise). Biogeosciences. **15**: 4215–4232. doi:10.5194/BG-15-4215-2018

Bonnet, S., and others. 2022. Diazotrophs are overlooked contributors to carbon and nitrogen export to the deep ocean. ISME J. **17**: 47–58. doi:10.1038/s41396-022-01319-3

Bonnet, S., J. Dekaezemacker, K. A. Turk-Kubo, T. Moutin, R. M. Hamersley, O. Grosso, J. P. Zehr, and D. G. Capone. 2013. Aphotic N_2 fixation in the eastern tropical South Pacific Ocean. PLoS One. **8**: e81265. doi:10.1371/JOURNAL.PONE.0081265

Bopp, L., and others. 2022. Diazotrophy as a key driver of the response of marine net primary productivity to climate change. Biogeosciences **19**: 4267–4285. doi:10.5194/bg-19-4267-2022

Böttjer, D., J. E. Dore, D. M. Karl, R. M. Letelier, C. Mahaffey, S. T. Wilson, J. Zehr, and M. J. Church. 2017. Temporal variability of nitrogen fixation and particulate nitrogen export at Station ALOHA. Limnol. Oceanogr. **62**: 200–216. doi:10.1002/LNO.10386

Caffin, M., H. Berthelot, V. Cornet-Barthaux, A. Barani, and S. Bonnet. 2018. Transfer of diazotroph-derived nitrogen to the planktonic food web across gradients of N_2 fixation activity and diversity in the western tropical South Pacific Ocean. Biogeosciences **15**: 3795–3810. doi:10.5194/bg-15-3795-2018

Capone, D. G., J. P. Zehr, H. W. Paerl, B. Bergman, and E. J. Carpenter. 1997. Trichodesmium, a globally significant marine cyanobacterium. Science (80-). **276**: 1221–1229. doi:10.1126/SCIENCE.276.5316.1221

Caron, D., and others. 1995. The contribution of microorganisms to particulate carbon and nitrogen in surface waters of the Sargasso Sea near Bermuda. Elsevier.

Chen, Y. B., J. P. Zehr, and M. Mellon. 1996. Growth and nitrogen fixation of the diazotrophic filamentous nonheterocystous cyanobacterium *Trichodesmium* sp. IMS 101 in defined media: Evidence for a circadian rhythm. J. Phycol. **32**: 916–923. doi:10.1111/j.0022-3646.1996.00916.x

Dekaezemacker, J., and S. Bonnet. 2011. Sensitivity of N_2 fixation to combined nitrogen forms (NO^{-3} and NH^{+4}) in two strains of the marine diazotroph *Crocosphaera watsonii* (Cyanobacteria). Mar. Ecol. Prog. Ser. **438**: 33–46. doi:10.3354/meps09297

Engel, A. 2000. The role of transparent exopolymer particles (TEP) in the increase in apparent particle stickiness (α) during the decline of a diatom bloom. Journal of Plankton Research. **22**(3): 485–497. doi:10.1093/plankt/22.3.485

Engel, A. 2004. Distribution of transparent exopolymer particles (TEP) in the Northeast Atlantic Ocean and their potential significance for aggregation processes. Deep-Sea Res. Part I Oceanogr. Res. Pap. **51**: 83–92. doi:10.1016/j.dsr.2003.09.001

Engel, A. 2009. Determination of marine gel particles. In Practical guidelines for the analysis of seawater: 137–154. CRC Press.

Farnelid, H., K. Turk-Kubo, H. Ploug, J. E. Ossolinski, J. R. Collins, B. A. S. Van Mooy, and J. P. Zehr. 2019. Diverse diazotrophs are present on sinking particles in the North Pacific Subtropical *Gyre*. ISME J. **13**: 170–182. doi:10.1038/s41396-018-0259-x

Freibott, A., L. Linacre, and M. R. Landry. 2014. A slide preparation technique for light microscopy analysis of ciliates preserved in acid Lugol's fixative. Limnol. Oceanogr.: Methods **12**: 54–62. doi:10.4319/lom.2014.12.54

Gruber, N., and J. N. Galloway. 2008. An earth-system perspective of the global nitrogen cycle. Nature **451**: 293–296. doi:10.1038/nature06592

Guigue, C., M. Tedetti, D. H. Dang, J. U. Mullot, C. Garnier, and M. Goutx. 2017. Remobilization of polycyclic aromatic hydrocarbons and organic matter in seawater during sediment resuspension experiments from a polluted coastal environment: Insights from Toulon Bay (France). Environ. Pollut. **229**: 627–638. doi:10.1016/J.ENVPOL.2017.06.090

Held, N. A., and others. 2022. Dynamic diel proteome and daytime nitrogenase activity supports buoyancy in the cyanobacterium Trichodesmium. Nat. Microbiol. **7**: 300–311. doi:10.1038/s41564-021-01028-1

Hutchins, D. A., and F. Fu. 2017. Microorganisms and ocean global change. Nat. Microbiol. **2**: 1–11. doi:10.1038/nmicrobiol.2017.58

Iversen, M. H., and M. L. Robert. 2015. Ballasting effects of smectite on aggregate formation and export from a natural plankton community. Mar. Chem. **175**: 18–27. doi:10.1016/J.MARCHEM.2015.04.009

Jackson, G. A. 1990. A model of the formation of marine algal flocs by physical coagulation processes. Deep-Sea Res. Part A Oceanogr. Res. Pap. **37**: 1197–1211. doi:10.1016/0198-0149(90)90038-W

Johnson, C. P., X. Li, and B. E. Logan. 1996. Settling velocities of fractal aggregates. Environ. Sci. Technol. **30**: 1911–1918. doi:10.1021/ES950604G

Karl, D. M., and others. 2003. Temporal studies of biogeochemical processes determined from ocean time-series observations during the JGOFS era. Ocean Biogeochem: 239–267. doi:10.1007/978-3-642-55844-3_11

Karl, D. M., D. V. Hebel, K. Björkman, and R. M. Letelier. 1998. The role of dissolved organic matter release in the productivity of the oligotrophic North Pacific Ocean. Limnol. Oceanogr. **43**: 1270–1286. doi:10.4319/LO.1998.43.6.1270

Karl, D. M., M. J. Church, J. E. Dore, R. M. Letelier, and C. Mahaffey. 2012. Predictable and efficient carbon sequestration in the North Pacific Ocean supported by symbiotic nitrogen fixation. Proc. Natl. Acad. Sci. **109**: 1842–1849. doi:10.1073/pnas.1120312109

Kiørboe, T., P. Tiselius, B. Mitchell-Innes, J. L. S. Hansen, A. W. Visser, and X. Mari. 1998. Intensive aggregate formation with low vertical flux during an upwelling-induced diatom bloom. Limnol. Oceanogr. **43**: 104–116. doi:10.4319/LO.1998.43.1.0104

Knapp, A. N., D. M. Sigman, and F. Lipschultz. 2005. N isotopic composition of dissolved organic nitrogen and nitrate at the Bermuda Atlantic time-series study site. Global Biogeochem. Cycles. **19**: 1–15. doi:10.1029/2004GB002320/FORMAT/PDF

Knapp, A. N., K. M. Mccabe, O. Grosso, N. Leblond, T. Moutin, and S. Bonnet. 2018. Distribution and rates of nitrogen fixation in the western tropical South Pacific Ocean constrained by nitrogen isotope budgets. Biogeosciences **15**: 2619–2628. doi:10.5194/bg-15-2619-2018

Laurenceau-Cornec, E. C., T. W. Trull, D. M. Davies, C. L. De La Rocha, and S. Blain. 2015. Phytoplankton morphology controls on marine snow sinking velocity. Mar. Ecol. Prog. Ser. **520**: 35–56. doi:10.3354/meps11116

Laurenceau-Cornec, E. C., F. A. C. Le Moigne, M. Gallinari, B. Moriceau, J. Toullec, M. H. Iversen, A. Engel, and C. L. De La Rocha. 2019. New guidelines for the application of Stokes' models to the sinking velocity of marine aggregates. Limnol. Oceanogr. **65**: 1264–1285. doi:10.1002/lno.11388

Le Moigne, F. A. C., M. Gallinari, E. Laurenceau, and C. L. De La Rocha. 2013. Enhanced rates of particulate organic matter remineralization by microzooplankton are diminished by added ballast minerals. Biogeosciences. **10**: 5755–5765. doi:10.5194/bg-10-5755-2013

Loescher, C. R., and others. 2014. Facets of diazotrophy in the oxygen minimum zone waters off Peru. ISME J **8**: 2180–2192. doi:10.1038/ismej.2014.71

Luo, Y. W., and others. 2012. Database of diazotrophs in global ocean: Abundance, biomass and nitrogen fixation rates. Earth Syst. Sci. Data **4**: 47–73. doi:10.5194/ESSD-4-47-2012

Mari, X. 1999. Carbon content and C : N ratio of transparent exopolymeric particles (TEP) produced by bubbling exudates of diatoms. Mar. Ecol. Prog. Ser. **183**: 59–71. doi:10.3354/MEPS183059

Mari, X., and A. Burd. 1998. Seasonal size spectra of transparent exopolymeric particles (TEP) in a coastal sea and comparison with those predicted using coagulation theory. Mar. Ecol. Prog. Ser. **163**: 63–76. doi:10.3354/meps163063

Mari, X., F. Rassoulzadegan, C. P. D. Brussaard, and P. Wassmann. 2005. Dynamics of transparent exopolymeric particles (TEP) production by *Phaeocystis globosa* under N- or P-limitation: A controlling factor of the retention/export balance. Harmful Algae **4**: 895–914. doi:10.1016/j.hal.2004.12.014

Mari, X., U. Passow, C. Migon, A. B. Burd, and L. Legendre. 2017. Transparent exopolymer particles: Effects on carbon cycling in the ocean. Prog. Oceanogr. **151**: 13–37. doi:10.1016/j.pocean.2016.11.002

Moisander, P. H., T. Serros, R. W. Paerl, R. A. Beinart, and J. P. Zehr. 2014. Gammaproteobacterial diazotrophs and nifH gene expression in surface waters of the South Pacific Ocean. ISME J. **8**: 1962–1973. doi:10.1038/ismej.2014.49

Moore, J. K., K. Lindsay, S. C. Doney, M. C. Long, and K. Misumi. 2013. Marine ecosystem dynamics and biogeochemical cycling in the community earth system model [CESM1(BGC)]: Comparison of the 1990s with the 2090s under the RCP4.5 and RCP8.5 scenarios. J. Climate **26**: 9291–9312. doi:10.1175/JCLI-D-12-00566.1

Mulholland, M. R. 2007. The fate of nitrogen fixed by diazotrophs in the ocean. Biogeosciences **4**: 37–51. doi:10.5194/bg-4-37-2007

Pabortsava, K., and others. 2017. Carbon sequestration in the deep Atlantic enhanced by Saharan dust. Nat. Geosci. **10**: 189–194. doi:10.1038/ngeo2899

Passow, U. 2000. Formation of transparent exopolymer particles, TEP, from dissolved precursor material. Mar. Ecol. Prog. Ser. **192**: 1–11. doi:10.3354/meps192001

Passow, U. 2002. Transparent exopolymer particles (TEP) in aquatic environments. Prog. Oceanogr. **55**: 287–333. doi:10.1016/S0079-6611(02)00138-6

Passow, U., and A. L. Alldredge. 1995. A dye-binding assay for the spectrophotometric measurement of transparent exopolymer particles (TEP). Limnol. Oceanogr. **40**: 1326–1335. doi:10.4319/LO.1995.40.7.1326

Ploug, H., A. Terbrüggen, A. Kaufmann, D. Wolf-Gladrow, and U. Passow. 2010. A novel method to measure particle sinking velocity in vitro, and its comparison to three other in vitro methods. Limnol. Oceanogr.: Methods. **8**: 386–393. doi:10.4319/lom.2010.8.386

Poff, K. E., A. O. Leu, J. M. Eppley, D. M. Karl, and E. F. DeLong. 2021. Microbial dynamics of elevated carbon flux in the open ocean's abyss. Proc. Natl. Acad. Sci. USA. **118** (4): e2018269118. doi:10.1073/PNAS.2018269118

Riley, J. S., R. Sanders, C. Marsay, F. A. C. Le Moigne, E. P. Achterberg, and A. J. Poulton. 2012. The relative contribution of fast and slow sinking particles to ocean carbon export. Global Biogeochem. Cycles. **26**(1). doi:10.1029/2011GB004085

Rochelle-Newall, E. J., X. Mari, and O. Pringault. 2010. Sticking properties of transparent exopolymeric particles (TEP) during aging and biodegradation. J. Plankton Res. **32**: 1433–1442. doi:10.1093/PLANKT/FBQ060

Sarmiento, J. L., and others. 2004. Response of ocean ecosystems to climate warming. Global Biogeochem. Cycles. **18**(3). doi:10.1029/2003GB002134

Schindelin, J., C. T. Rueden, M. C. Hiner, and K. W. Eliceiri. 2015. The ImageJ ecosystem: An open platform for

biomedical image analysis. Mol. Reprod. Dev. **82**: 518–529. doi:10.1002/MRD.22489

Sohm, J. A., B. R. Edwards, B. G. Wilson, and E. A. Webb. 2011. Constitutive extracellular polysaccharide (EPS) production by specific isolates of *Crocosphaera watsonii*. Front. Microbiol. **2**: 1–9. doi:10.3389/fmicb.2011.00229

Subramaniam, A., and others. 2008. Amazon River enhances diazotrophy and carbon sequestration in the tropical North Atlantic Ocean. Proc. Natl. Acad. Sci. **105**: 10460–10465. doi:10.1073/PNAS.0710279105

Villareal, T. A. 1991. Nitrogen-fixation by the cyanobacterial symbiont of the diatom genus *Hemiaulus*. Mar. Ecol. Prog. Ser. **76**: 201–204. doi:10.3354/meps076201

Villareal, T. A., and E. J. Carpenter. 1994. Chemical composition and photosynthetic characteristics of *Ethmodiscus rex* (Bacillariophyceae): evidence for vertical migration. J. Phycol. **30**: 1–8. doi:10.1111/J.0022-3646.1994.00001.X

Walsby, A. E. 1978. The properties and buoyancy-providing role of gas vacuoles in *Trichodesmium* Ehrenberg. Br. Phycol. J. **13**: 103–116. doi:10.1080/00071617800650121

White, A. E., R. A. Foster, C. R. Benitez-Nelson, P. Masqué, E. Verdeny, B. N. Popp, K. E. Arthur, and F. G. Prahl. 2013. Nitrogen fixation in the Gulf of California and the eastern tropical North Pacific. Prog. Oceanogr. **109**: 1–17. doi:10.1016/J.POCEAN.2012.09.002

Zehr, J. P., J. B. Waterbury, P. J. Turner, J. P. Montoya, E. Omoregie, G. F. Steward, A. Hansen, and D. M. Karl. 2001. Unicellular cyanobacteria fix N_2 in the subtropical North Pacific Ocean. Nature **412**: 635–638. doi:10.1038/35088063

Acknowledgments

We would like to thank Xavier Mari and Carolina Cisternas-Novoa for their comments and valuable advice on the TEP section, and France Van Wambeke for her help in the experiments. Brahim Lamkadem (Alpes maintenance générale) is warmly thanked for the design and construction of the roller table. We also thank the two reviewers who helped significantly to improve this manuscript. F.E.A. Ababou was supported by a PhD scholarship from the Institut de Recherche pour le Developpement (IRD, ARTS). Funding for this research was provided by the TONGA project (Agence Nationale de la Recherche). S.B. was funded by IRD and F.A.C.L.M. by CNRS. The Calothrix strain has been isolated from the Noumea lagoon (New Caledonia, origin N°2617-2020/ARR/DDDT), contract registration N°APA_NCPS_2021_007.

Conflict of Interest

None declared.

Submitted 29 April 2022
Revised 16 September 2022
Accepted 17 December 2022

Associate editor: Laura Bristow